Revisiting the Pan Evaporation Trend in China From 1988-2017

Jiaju Shen[1], Hanbo Yang[1], Sien Li[2], Ziwei Liu[1], Yongqiang Cao[3], and Dawen Yang[1]

[1]Tsinghua University
[2]China Agricultural University
[3]Liaoning Normal University

November 24, 2022

Abstract

Pan evaporation decrease has been reported worldwide over them past decades. A recovery trend, even an increasing pan evaporation trend, has been recently found. Remarkably, most studies on Chinese pan evaporation change in China were based on simulations involving meteorological variables, including temperature, radiation (sunshine duration), wind speed and relative humidity, due to the pan evaporation observation inconsistency caused by the micropan (D20) replacement with large pans (E601) around 2002. In addition, it has been reported that a large-scale humidity sensor replacement across China has occurred since the 2000s, which can cause an underestimation of relative humidity and in turn leads to an inconsistency in simulated pan evaporation. Therefore, the recent pan evaporation trend independent of the observed relative humidity in China must be revisited. In this study, we complete the D20 pan evaporation from 1988 to 2017 according to E601 observations under the constant conversion coefficient assumption between the evaporation observations of these pans in the same month of every year at each station and conduct trend and attribution analysis through linear regression and PenPan-D20 model partial differential methods, respectively. A significant 2.68 mm/a/a upward pan evaporation trend (P<0.05) from 1988-2017 is revealed, primarily driven by the air temperature rise across China. Humidity sensor replacement causes an ˜1.3% relative humidity underestimation, producing nonnegligible pan evaporation trend simulation errors.

Revisiting the Pan Evaporation Trend in China From 1988-2017

Jiaju Shen[1], Hanbo Yang[1]*, Sien Li[2], Ziwei Liu[1], Yongqiang Cao[3], Dawen Yang[1]

1. State Key Laboratory of Hydro-Science and Engineering, Department of Hydraulic Engineering, Tsinghua University, Beijing 100084, China;
2. Center for Agricultural Water Research in China, China Agricultural University, Beijing, 100083, China;
3. School of Urban Planning and Environmental Science, Liaoning Normal University, Dalian, 116029, China.

* Correspondence to: Hanbo Yang; e-mail: yanghanbo@tsinghua.edu.cn.

Key Points:

- We complete a long-term D20 pan evaporation series from 1988-2017.
- Pan evaporation exhibits a 2.68 mm/a/a increasing trend from 1988-2017, mainly driven by air temperature increase.
- An ~1.3% underestimation occurs owing to the replacement of relative humidity sensors since the 2000s across China.

Abstract

Pan evaporation decrease has been reported worldwide over them past decades. A recovery trend, even an increasing pan evaporation trend, has been recently found. Remarkably, most studies on Chinese pan evaporation change in China were based on simulations involving meteorological variables, including temperature, radiation (sunshine duration), wind speed and relative humidity, due to the pan evaporation observation inconsistency caused by the micropan (D20) replacement with large pans (E601) around 2002. In addition, it has been reported that a large-scale humidity sensor replacement across China has occurred since the 2000s, which can cause an underestimation of relative humidity and in turn leads to an inconsistency in simulated pan evaporation. Therefore, the recent pan evaporation trend independent of the observed relative humidity in China must be revisited. In this study, we complete the D20 pan evaporation from 1988 to 2017 according to E601 observations under the constant conversion coefficient assumption between the evaporation observations of these pans in the same month of every year at each station and conduct trend and attribution analysis through linear regression and PenPan-D20 model partial differential methods, respectively. A significant 2.68 mm/a/a upward pan evaporation trend ($P<0.05$) from 1988-2017 is revealed, primarily driven by the air temperature rise across China. Humidity sensor replacement causes an ~1.3% relative humidity underestimation, producing nonnegligible pan evaporation trend simulation errors.

1. Introduction

Pan evaporation is an important indicator of the atmospheric evaporative demand (AED). It has been stated that the global mean surface air temperature has increased 0.13°C per decade over the last 50 years (*IPCC*, 2014). Moreover, a significant downward trend in pan evaporation has been widely reported over the past several decades, such as in China (*B Liu*, 2004; *H Yang and Yang*, 2012), India (*N. Chattopadhyay*, 1997; *Verma and Jadhav*, 2008), Africa (*Hoffman et al.*, 2011; *Oguntunde et al.*, 2012), New Zealand (*Roderick and Farquhar*, 2005), the United States (*Hobbins et al.*, 2004; *Peterson et al.*, 1995), Australia (*Roderick and Farquhar*, 2004), and Thailand (*Limjirakan and Limsakul*, 2012).

In recent years, studies have reported an upward trend in pan evaporation, which is in contrast to the downward trend found in the 1990s in certain regions of the world (Table 1). In Turkey, the pan evaporation trend from 1997 to 2015 exhibited a nonsignificant -0.07 mm/a/a decrease (*Yagbasan et al.*, 2020), which is in contrast to the upward trend from 1975 to 2006 (*Topaloglu et al.*, 2012). In Iran, a significant decreasing pan evaporation trend from 1995 to 2015 was found (*Shimi et al.*, 2020), while a 16 mm/a/a increase trend occurred from 1982 to 2003 (*Talaee et al.*, 2014). Mexico has also demonstrated a recovery trend since 1990, and certain regions have even shown an upward trend (*Brena-Naranjo et al.*, 2017; *Ruiz-Alvarez et al.*, 2019). Additionally, a similar upward trend has been detected in Australia, parts of the U.S., Uruguay and other regions (*Abtew et al.*, 2011; *Stephens et al.*, 2018; *Vicente-Serrano et al.*, 2018). It seems that the pan evaporation trend has changed at the end of the twentieth century.

(Table 1 near here)

In China, a decreasing pan evaporation trend from the 1960s-2000s has also been reported (*B Liu*, 2004; *M Liu et al.*, 2010; *H Yang and Yang*, 2012), and this has been speculated to be caused by decreases in solar radiation and wind speed. However, decreases in wind speed, as well as in solar radiation, are limited (*McVicar et al.*, 2012). This implies that the decreasing trend in pan evaporation will unlikely be sustained. In fact, the pan evaporation trend has already exhibited a recovery trend since the 1990s because the rising air temperature offsets the influences of the decreasing wind speed and solar radiation in China (*Cao W*, 2015; *X Liu et al.*, 2011; *T Wang et al.*, 2017). However, due to the replacement of the D20 micropan with the large E601 pan around 2002, D20 pan evaporation observation data are missing after 2002. Although the E601 pan provides alternative pan evaporation data, the data are discontinuous and inconsistent with D20 pan data (*K Wang et al.*, 2019; *T Wang et al.*, 2017; *Xiong et al.*, 2012). Therefore, regarding the change in pan evaporation in China, most studies have only focused on the trend before 2002. To examine the recent trend, previous studies have adopted the pan evaporation simulation method using the PenPan model (*T Wang et al.*, 2017) or the Penman-Monteith equation (*X Liu et al.*, 2011). Remarkably, these models require the relative humidity as input. However, large-scale replacement of humidity sensors has occurred in Chinese meteorological stations since the 2000s, which can lead to inconsistencies in relative humidity observations. For instance, Yu et al. (2008) found that an average 2.2% underestimation occurred at 17 representative stations across China. In addition, Yang et al. (2014) also reported that replacement has led to a greater than 2% jump in 64% of all cases in Hubei Province. Consequently, this underestimation will cause an overestimation in the simulated pan evaporation, which in turn lead to an overestimation of its trend. Therefore, it is important to investigate pan evaporation trends independent of the observed humidity in recent years.

To revisit the recent pan evaporation trend in China and understand its attribution, this study therefore collects pan evaporation observation data of these two pans across China and complete a long-term continuous and consistent D20 pan evaporation dataset based on the relationship between the measured pan evaporation data of these two pans, namely, the D20 and E601 pans. Furthermore, this study analyzes the trend and attribution of its recent change using linear regression and the partial differential of the PenPan-D20 model (*H Yang and Yang*, 2012), respectively.

2. Data and Methods

2.1 Data

Daily meteorological data from 1988-2017, including the air temperature (T), sunshine duration (SSD), relative humidity (RH), wind speed (U) and pan evaporation, were collected from 756 meteorological stations of the China Meteorological Administration (CMA). Monthly values were calculated as the arithmetic mean of the daily values when no fewer than 25 daily observations were available in a month. The annual average was then calculated as the arithmetic mean of the monthly values when 12 monthly values were available.

Specifically, there are two types of pans widely used to measure pan evaporation in China. The first type is the D20 small evaporation pan, of which almost full records are available before the 2000s. However, it was replaced by the second pan type, the E601 pan, in 2002. In addition, the E601 pan does not function in winter because the water inside may be frozen. The number of usable stations with available monthly D20 and E601 data is shown in Figure 1. The above causes a discontinuity and inconsistency in pan evaporation data. The solution to this problem is introduced in Section 2.2.1.

(Figure 1 near here)

The net radiation (R_n) was calculated by the SSD and location based on the empirical equation recommended by the Food and Agriculture Organization (FAO) (*Allen et al.*, 1998). Details are provided in Section 2.2.2.

(Figure 2 near here)

2.2 Method

2.2.1 Deriving a Long-term Monthly D20 Pan Evaporation

Due to the replacement of the D20 pan with the E601 pan around 2002 in China, the pan evaporation observation records are discontinuous and inconsistent (*K Wang et al.*, 2019; *Xiong et al.*, 2012). We applied a simple conversion coefficient method to calculate the D20 pan evaporation from the E601 pan evaporation. In this method, we (1) chose meteorological stations that provide both D20 and E601 pan data during the same period, mainly from 1988-2001; (2) calculated the two-type evaporation pan conversion coefficient ($k = \frac{E(\mathrm{D20})}{E(\mathrm{E601})}$) at the monthly scale, and in this step, we randomly chose ten years of monthly data to calculate k, and the remaining four years of data were reserved for validation purposes; and (3) calculated the D20 pan evaporation as $E(\mathrm{D20}) = k * E(\mathrm{E601})$ when D20 pan data were missing and E601 pan data were available. Finally, we obtained a D20 pan evaporation dataset, which includes full monthly data covering 469 stations (as shown in Figure 2).

2.2.2 Net Radiation Estimation

The net radiation R_n can be estimated based on the empirical equation recommended by the FAO (*Allen et al.*, 1998) as follows:

$$R_n = R_{ns} - R_{nl} \tag{1}$$

where R_{ns} is the incoming net shortwave radiation (MJ m^{-2} day^{-1}) and R_{nl} is the outgoing net longwave radiation (MJ m^{-2} day^{-1}).

$$R_{nl} = \sigma T^4 \left(0.34 - 0.14\sqrt{e_a}\right)\left(1.35\frac{R_s}{R_{s0}} - 0.35\right) \tag{2}$$

$$R_{ns} = (1-\alpha)R_{sp} \tag{3}$$

where α is the pan albedo, with $\alpha = 0.14$ recommended for pans (*Roderick et al.*, 2007; *Rotstayn et al.*, 2006), σ is the Stefan-Boltzmann constant (4.903×10^{-9} MJ K^{-4} m^{-2} day^{-1}) and R_{sp} is the incoming shortwave radiation of the D20 pan, which approximately equals $2.5R_s$ (*H Yang and Yang*, 2012).

$$R_s = (a_s + b_s\frac{SSD}{N})R_a \tag{4}$$

$$R_{s0} = (a_s + b_s)R_a \tag{5}$$

where R_s is the shortwave radiation (MJ m^{-2} day^{-1}), R_{s0} is the clear-sky shortwave radiation (MJ m^{-2} day^{-1}), a_s expresses the fraction of extraterrestrial radiation reaching the earth on overcast days (SSD = 0) and $a_s + b_s$ is the fraction of extraterrestrial radiation reaching the earth on clear days (SSD = N). The values of a_s = 0.25 and b_s = 0.50 were adopted when no observation radiation data were available. R_a is the extraterrestrial radiation, which is determined by the meteorological station information (MJ m^{-2} day^{-1}).

2.2.3 Trend Analysis

Trend analysis of the pan evaporation and climate variables was conducted by the linear regression method. Furthermore, the Mann–Kendall (MK) nonparametric test (*Kendall*, 1975; *Mann*, 1945) was applied to detect the significance of trends. Regarding the effect due to the replacement of humidity sensors, it has been found that a 2.2% underestimation occurs at 17 representative stations across China (*Jun and Rong*, 2008). Therefore, we also revised the annual RH series since 2004 by adding values of 1% and 2% across China and determined the resultant trends from 1988-2017.

2.2.4 Attribution Analysis

The pan evaporation is a comprehensive variable integrating the effects of several meteorological elements, such as RH, SSD (which represents solar radiation), air temperature and wind speed. To reveal the causes for the observed pan evaporation changes, we adopted the partial differential equation of the PenPan-D20 model (*H Yang and Yang*, 2012). According to the PenPan-D20 model, the pan evaporation determined by the D20 pan (E_{pan}) can be estimated as:

$$E_{pan} = \frac{\Delta}{\Delta+\alpha\gamma} \cdot \frac{R_n}{\lambda} + \frac{\alpha\gamma}{\Delta+\alpha\gamma} \cdot f_q(U) \cdot \frac{D}{\lambda} \quad (6)$$

In Eq. (6), Δ is the slope of the saturation vapor pressure curve at a given T (kPa °C^{-1}), λ is the latent heat of vaporization (MJ kg^{-1}), γ is the psychometric constant (kPa °C^{-1}), R_n is the net radiation flux (MJ m^{-2} day^{-1}) estimated by the empirical equation recommended by the FAO (*Allen et al.*, 1998), $f_q(U)$ is the vapor transfer function (kg m^{-2} day^{-1} kPa) equal to $5.4 \times (1 + 0.73U)$, D is the vapor pressure deficit (kPa), and α is defined as the ratio of the effective surface areas for heat and water vapor transfer, which equals 5 for the D20 pan.

According to the partial differential equation of Eq. (6), the attribution analysis is quantitatively given as follows:

$$\frac{dE_{pan}}{dt} = \frac{\partial E_{pan}}{\partial RH} \cdot \frac{dRH}{dt} + \frac{\partial E_{pan}}{\partial SSD} \cdot \frac{dSSD}{dt} + \frac{\partial E_{pan}}{\partial T} \cdot \frac{dT}{dt} + \frac{\partial E_{pan}}{\partial U} \cdot \frac{dU}{dt}$$
$$= \varepsilon_1 \cdot \frac{dRH}{dt} + \varepsilon_2 \cdot \frac{dSSD}{dt} + \varepsilon_3 \cdot \frac{dT}{dt} + \varepsilon_4 \cdot \frac{dU}{dt}$$
$$= RH^* + SSD^* + T^* + U^* \quad (7)$$

where RH^*, SSD^*, T^* and U^* represent the contributions of RH, SSD, T and U, respectively, to the change in E_{pan}, and coefficients $\varepsilon_1, \varepsilon_2, \varepsilon_3$, and ε_4 are calculated as $\varepsilon_1 = \frac{\partial E_{pan}}{\partial RH}|_{X=\bar{X}}$, $\varepsilon_2 = \frac{\partial E_{pan}}{\partial SSD}|_{X=\bar{X}}$, $\varepsilon_3 = \frac{\partial E_{pan}}{\partial T}|_{X=\bar{X}}$, and $\varepsilon_4 = \frac{\partial E_{pan}}{\partial U}|_{X=\bar{X}}$, respectively, with $X = \bar{X}$ representing $RH = \overline{RH}$, $SSD = \overline{SSD}$, $T = \bar{T}$ or $U = \bar{U}$ and the overline indicating the mean value. Moreover, the maxima among RH^*, SSD^*, T^* and U^* are considered as the controlling climatic factor of the pan evaporation trend. Similar methods have been widely applied to attribute the change in pan evaporation in previous studies (*X Liu et al.*, 2011; *Roderick et al.*, 2007)

3. Results

3.1 Conversion Coefficient Method for the D20 Pan Evaporation

Table 2 lists the standard deviation in the conversion coefficient for the same month of every year at each station according to the observations. From February to November, the standard deviation is smaller than 0.2 at more than 90%, even up to 98%, of the stations. Even though January exhibits the largest standard deviation, the standard deviation is smaller than 0.4 at 98% of all stations. This indicates that the interannual variation in the conversion coefficient is small. The mean conversion coefficient demonstrates an obvious seasonal variation, which is larger in summer than in winter. More detailed information has been provided in the Supporting Information.

(Table 2 near here)

(Figure 3 near here)

Figure 3 shows that the monthly D20 observation data and conversion coefficient method-calculated D20 data exhibit a good fit at all 469 stations. The best-fit regression function in calibration is y=0.99x+16.67, with R^2=0.97 and root mean square error (RMSE)=13.55 mm/month, and the best-fit regression function in validation is y=0.98x+36.72, with R^2=0.96 and RMSE=14.63 mm/month. This indicates that the D20 pan evaporation data can be extended to 2017 according to the E601 data with the conversion coefficient method.

3.2 Trends in the Meteorological Variables

Figure 4 shows that for China as a whole, a significant -0.11%/a (P<0.001) trend in the original RH, a significant -1.6 h/a (P<0.05) trend in the SSD, a significant 0.03°C/a (P<0.001) increase in the air temperature, and a significant 0.005 m/s (P<0.001) decline in the wind speed occurred. Figure 4(a) shows the trends in the modified RH data. There was no significant downward trend in the modified-2% RH data, and a 0.06%/a significant (P=0.05) decline was found in the modified-1% RH data.

(Figure 4 near here)

3.3 Trend in Pan Evaporation

Figure 5(a) shows that the pan evaporation in China from 1988 to 2017 experiences a significant 2.68 mm/a/a (P<0.005) upward trend. It is found that 1997 represents a mutation point, after which the pan evaporation trend significantly increases. The trend before the mutation point, i.e., from 1988-1997, shows a nonsignificant 4.38 mm/a/a increasing trend. The trend from 1998-2017 exhibits a nonsignificant 0.07 mm/a/a slight downward trend. Figure 5(b) shows that among 469 meteorological stations, 148 stations reveal a significant (P<0.05) increasing trend, while 64 stations exhibit a significant (P<0.05) decreasing trend. In addition, in regard to the spatial distribution, the downward trend mainly occurs in the North China Plain, while the stations with significant upward trends are concentrated in southern China.

(Figure 5 near here)

3.4 Attribution Analysis

Figure 6 shows that E_{pan}, calculated with the original RH data, exhibited a significant (P<0.001) increase of 4.14 mm/a/a from 1988 to 2017. This increase amplitude is larger than that found based on the derived D20 pan evaporation dataset.

When using the modified-1% relative humidity (blue line), the E_{pan} shows a significant (P<0.001) 3.13 mm/a/a upward trend, while E_{pan} derived from the modified-2% relative humidity (the red line) significantly (P<0.01) increases at 2.11 mm/a/a. In summary, the trend in the observed pan evaporation is higher than that in the modified-2% relative humidity but lower than that in the modified-1% relative humidity.

(Figure 6 near here)

Table 3 summarizes the contribution coefficients (ε) of the above four meteorological elements and the contributions of RH, SSD, T and U to the annual E_{pan} trends based on nationwide averages. The increasing air temperature contributes a 4.66 mm/a/a increase to E_{pan}, the most among the four climatic factors. In contrast, the decline in wind speed is primarily responsible for a reduction (average: 2.64 mm/a/a) in E_{pan}. Moreover, the decline in SSD also contributes to a decrease of 0.29 mm/a/a to the E_{pan} trend. Considering the impact of RH on pan evaporation, a comparison of the original results to the modified results is given in Table 3. The decline in the original RH data, modified-1% relative humidity, and the modified-2% relative humidity led to increases in pan evaporation of 2.02, 1.13 and 0.24 mm/a/a, respectively.

(Table 3 near here)

Figure 7 shows the controlling climatic factor of the pan evaporation change at the 469 stations. The wind speed decreased at 344 stations, and the air temperature increased at 116 stations. In addition, RH decreased at 4 stations and SSD decreased at 5 stations. Spatially, the wind speed acts as the controlling climatic factor across the whole China, while the air temperature is the controlling climatic factor mainly in the southern region of China.

(Figure 7 near here)

4. Discussion

4.1 Trend in Pan Evaporation

We extended the Chinese monthly D20 pan evaporation series to 2017 according to the acquired E601 observations and found a 2.68 mm/a/a upward trend from

1988-2017. This trend differs from the downward trends found before the 2000s, such as the 1.7 mm/a/a decrease from 1955-2001 (*M Liu et al.*, 2010), the 2.6 mm/a/a decrease from 1960-1993 (*Cao W*, 2015) and the 3.1 mm/a/a decrease from 1961-2001 (*H Yang and Yang*, 2012). In addition, similar upward trends in recent years have also been detected in previous studies, such as the 4.3 mm/a/a increase from 1994-2013 (*Cao W*, 2015) and the 7.9 mm/a/a increase from 1992-2007 (*X Liu et al.*, 2011). This indicates a recovery tendency of the pan evaporation across China in recent years. Remarkably, as shown in Figure 5(a), this upward trend becomes flat after 1997. Moreover, the decreasing trends of the RH, SSD and wind speed are consistent with those found in previous studies (*Jiang et al.*, 2010; *Li and Fu*, 2012; *Xie et al.*, 2011; *Y Yang et al.*, 2009).

Although the increasing trend detected in our study is similar to that reported in previous studies based on the simulated pan evaporation values (*X Liu et al.*, 2011; *K Wang et al.*, 2019; *T Wang et al.*, 2017), it should be noted that there is a significant difference in the amplitude of the trends, as indicated in Table 4. For instance, Wang et al. (2017) found a 4.3 mm/a/a trend from 1994-2014, while the trend based on our D20 dataset was 1.4 mm/a/a during the same period. We also adopted the reanalysis D20 dataset published by Wang et al. (2019) and determined a 10.14 mm/a/a increase from 1992-2007 and a 5.21 mm/a/a increase from 1994-2014. Meanwhile, the pan evaporation trend simulated by the PenPan-D20 model in our study showed a 4.14 mm/a/a increase from 1988-2017, a 9.09 mm/a/a increase from 1992-2007 and a 3.07 mm/a/a increase from 1994-2014. In summary, the pan evaporation trend simulated using the RH data is generally higher than the trend derived from the D20 dataset (Table 4). It is proposed that the replacement of humidity sensors since the 2000s across China leads to RH underestimation, which in turn causes an overestimation in simulated pan evaporation values after 2000 and an overestimation of the trend.

(Table 4 near here)

Regarding the attribution of the pan evaporation change, this study reveals an ~-2.6 mm/a/a contribution of the decreasing wind speed from 1988-2017, and a similar contribution (-2.7 mm/a/a) of the decreasing wind speed from 1961-2001 was reported by Yang and Yang (2012). In contrast, we find that the increasing air temperature plays a dominant role from 1988-2017 at the national scale, while Yang and Yang (2012) reported that the declining solar radiation and decreasing wind speed dominated the pan evaporation decrease from 1961-2001.

In addition, our results reveal an interesting phenomenon in which, at most stations with an increasing pan evaporation, the decreasing wind speed is the controlling factor. In contrast, the decreasing pan evaporation before the 2000s has been attributed to the decline in wind speed at most stations in China in previous studies (*M Liu et al.*, 2010; *H Yang and Yang*, 2012). Table 5 shows the attributions of the pan evaporation change at seven typical stations where the pan evaporation change is controlled by the wind speed. At 4 stations (i.e., 53963, 54186, 55279 and 56586), the pan evaporation shows an increasing trend, but the declining wind speed exerts the largest impact. This phenomenon is caused by the overall positive contribution of the RH and air temperature exceeding the negative contribution of the wind speed and SSD.

(Table 5 near here)

4.2 Inconsistencies in Relative Humidity Observations

(Figure 8 near here)

Figure 8 shows that the bias of the annual pan evaporation between the observations and estimation by the PenPan-20 model is 43.09 mm/a during the period from 1988-2003 and 65.81 mm/a during the period from 2004-2017. It is assumed that the bias during the former period is caused by the uncertainty in the PenPan-20 model, and the bias during the latter period is caused by both the model uncertainty and replacement of humidity sensors. Consequently, the effect of the replacement of evaporation pans is estimated as 22.72 (= 65.81 – 43.09) mm/a. As indicated in Table 3, a 1% change in RH leads to a 17.90 mm/a change in pan evaporation, i.e., ε_1 =17.90 mm/a/%. Therefore, the inconsistency caused by the replacement of humidity sensors is calculated as 23.54/ (-17.90) = -1.3%. A previous study (*Z B Yang et al.*, 2014) reported that 18 out of 28 sensor replacements caused a greater than 2% inconsistency in RH observations in Hubei Province, with an average of 3.4%. This indicates that the inconsistency can be estimated as 3.4%×18/28 = 2.2%. In addition, Yu et al. (2008) found an average 2.2% underestimation occurred at 17 representative stations across China, which approximately agrees with our results. Therefore, it is deduced that the large-scale replacement of humidity sensors has led to an ~1.3% RH underestimation since 2004 across China. Consequently, when focusing on issues related to humidity trends in China, the effects of instrument replacement are nonnegligible. Furthermore, the inconsistency caused by instrument replacement should be considered when determining the trends in the simulated potential evaporation, reference crop evapotranspiration, as well as actual evaporation.

4.3 Uncertainty

In this study, the conversion coefficient method is proposed based on the assumption that a constant conversion coefficient applies between the evaporation data of the above two pans in the same month of every year at each station. This ignores the possible change in conversion coefficient caused by climate change. As a 2.2% RH underestimation across China was found by Yu et al. (2008), we compared the trend of the modified-2% (Figure 6) to that of the D20 data derived with the conversion coefficient method (Figure 5(a)). Similar trends were observed, namely, 2.11 mm/a/a for the modified-2% and 2.68 mm/a/a for the D20 data. Therefore, to a certain extent, this verifies the applicability of the conversion coefficient method in the determination of pan evaporation trends.

We adopted the PenPan-D20 model to simulate the D20 pan evaporation and applied its differential equation (Eq. (7)) to conduct attribution analysis. In the PenPan-D20 model, to estimate the incoming shortwave radiation, Yang and Yang (2012) suggested $R_{\mathrm{sp}} = \left[P_{\mathrm{rad}} f_{\mathrm{dir}} + 2(1 - f_{\mathrm{dir}}) + 2\alpha_{\mathrm{g}}\right] R_{\mathrm{s}}$, where the pan evaporation factor P_{rad} is related to the latitude, f_{dir} is the fraction of direct radiation, and α_{g} is the surface albedo. In theory, the above three parameters vary at the different stations. Because most stations do not provide observations of the direct and diffuse radiation and surface albedo, we used an average value of $R_{\mathrm{sp}} = 2.5 R_{\mathrm{s}}$ at all stations. Their spatial variations possibly generate some uncertainty, which requires further study according to more data.

5. Conclusion

In this study, we generate a long-term D20 pan evaporation dataset from 1988 to 2017 assuming that the conversion coefficient between the evaporation data of the considered two types of pans remains constant in the same month of every year at each station. Based on this dataset, we found a 2.68 mm/a/a increasing trend ($P<0.05$) in the pan evaporation during this period across China, which was dominated by the rising air temperature. Among the 469 individual stations, the pan evaporation exhibited a significant ($P<0.05$) increasing trend at 148 stations, and a significant ($P<0.05$) decreasing trend was observed at 64 stations. The controlling factor of this change was the decreasing wind speed at 344 stations and the rising air temperature at 116 stations. Remarkably, at certain stations with an increasing pan evaporation trend, the decreasing wind speed exerted the largest impact, and this phenomenon was caused by the overall positive contribution of the RH and air temperature exceeding the negative contribution of the wind speed and SSD. Comparing the pan evaporation trends of this dataset and the simulation dataset obtained with the PenPan-D20 model, we found an ~1.3% RH underestimation caused by the large-scale replacement of humidity sensors since the 2000s across China, and this underestimation should be considered when determining trends in potential evaporation, reference crop evapotranspiration, as well as actual evaporation.

Acknowledgments

This research was supported by funding from the National Natural Science Foundation of China (Grant No. 51979140) and the Program of the Joint Institute of Internet of Water and Digital Water Governance, Tsinghua-Ningxia Yinchuan (Grant No. sklhse-2020-Iow04). We are very grateful to the China Meteorological Data Sharing Service System for providing the meteorological data.

References

Abtew, W., J. Obeysekera, and N. Iricanin (2011), Pan evaporation and potential evapotranspiration trends in South Florida, *Hydrological Processes*, *25*(6), 958-969, doi:10.1002/hyp.7887.

Allen, R. G., L. S. Pereira, D. Raes, and M. Smith (1998), *Crop evapotranspiration-Guidelines for computing crop water requirements-FAO Irrigation and drainage paper 56*, D05109 pp., FAO, Rome.

Brena-Naranjo, J. A., M. A. Laverde-Barajas, and A. Pedrozo-Acuna (2017), Changes in pan evaporation in Mexico from 1961 to 2010, *International Journal of Climatology*, *37*(1), 204-213, doi:10.1002/joc.4698.

Cao W, D. C. F., Shen S H (2015), Inter-decadal breakpoint in potential evapotranspiration trends and the main causes in China during the period 1971—2010, *Acta Ecologica Sinica*, *35*(15), 5085-5094.

Hobbins, M., J. Ramirez, and T. Brown (2004), Trends in pan evaporation and actual evapotranspiration across the conterminous U.S.: Paradoxical or complementary?, *Geophysical Research Letters*, *31*, doi:10.1029/2004GL019846.

Hoffman, M. T., M. D. Cramer, L. Gillson, and M. Wallace (2011), Pan evaporation and wind run decline in the Cape Floristic Region of South Africa (1974–2005): implications for vegetation responses to climate change, *Climatic Change*, *109*(3-4), 437-452, doi:10.1007/s10584-011-0030-z.

IPCC (2014), *Climate Change 2014: Synthesis Report. Contribution of Working Groups I, II and III to the Fifth Assessment Report of the Intergovernmental Panel on Climate Change*, 151 pp pp., Geneva, Switzerland.

Jiang, Y., Y. Luo, Z. Zhao, and S. Tao (2010), Changes in wind speed over China during 1956-2004, *Theoretical Applied Climatology*, *99*(3-4), 421-430.

Jun, Y., and M. Rong (2008), Research on the Cause of Difference between AWS- and MAN- Relative Humidity Observations, *METEOROLOGICAL MONTHLY*, *34*(12), 97-102.

Kendall, M. G. (1975), *Rank Correlation Measures*, Charles Griffin, London.

Li, H., and Z. Fu (2012), Sunshine duration's trend behavior based on EEMD over China in 1956-2005, *Acta Scientiarum Naturalium Universitatis Pekinensis*, *48*(3), 393-398.

Limjirakan, S., and A. Limsakul (2012), Trends in Thailand pan evaporation from 1970 to 2007, *Atmospheric Research*, *108*, 122-127, doi:10.1016/j.atmosres.2012.01.010.

Liu, B. (2004), A spatial analysis of pan evaporation trends in China, 1955–2000, *Journal of Geophysical Research*, *109*(D15), doi:10.1029/2004jd004511.

Liu, M., Y. Shen, Y. Zeng, and C. Liu (2010), Trend in pan evaporation and its attribution over the past 50 years in China, *Journal of Geographical Sciences*, *20*(4), 557-568, doi:10.1007/s11442-010-0557-3.

Liu, X., Y. Luo, D. Zhang, M. Zhang, and C. Liu (2011), Recent changes in pan-evaporation dynamics in China, *Geophysical Research Letters*, *38*(13), n/a-n/a, doi:10.1029/2011gl047929.

Mann, H. B. (1945), NONPARAMETRIC TESTS AGAINST TREND, *Econometrica*, *13*(3), 245-259, doi:10.2307/1907187.

McVicar, T. R., et al. (2012), Global review and synthesis of trends in observed terrestrial near-surface wind speeds: Implications for evaporation, *Journal of Hydrology*, *416-417*, 182-205, doi:10.1016/j.jhydrol.2011.10.024.

N. Chattopadhyay, M. H. (1997), Evaporation and potential evapotranspiration in India under conditions of recent and future climate change, *Agricultural and Forest Meteorology*, *87*, 55-73.

Oguntunde, P. G., B. J. Abiodun, O. J. Olukunle, and A. A. Olufayo (2012), Trends and variability in pan evaporation and other climatic variables at Ibadan, Nigeria, 1973-2008, *Meteorological Applications*, *19*(4), 464-472, doi:10.1002/met.281.

Peterson, T. C., V. S. Golubev, and P. Y. Groisman (1995), Evaporation losing its strength, *Nature*, *377*(6551), 687-688, doi:10.1038/377687b0.

Roderick, M. L., and G. D. Farquhar (2004), Changes in Australian pan evaporation from 1970 to 2002, *International Journal of Climatology*, *24*(9), 1077-1090, doi:10.1002/joc.1061.

Roderick, M. L., and G. D. Farquhar (2005), Changes in New Zealand pan evaporation since the 1970s, *International Journal of Climatology*, *25*(15), 2031-2039, doi:10.1002/joc.1262.

Roderick, M. L., L. D. Rotstayn, G. D. Farquhar, and M. T. Hobbins (2007), On the attribution of changing pan evaporation, *Geophysical Research Letters*, *34*(17), doi:10.1029/2007gl031166.

Rotstayn, L. D., M. L. Roderick, and G. D. Farquhar (2006), A simple pan-evaporation model for analysis of climate simulations: Evaluation over Australia, *Geophysical Research Letters*, *33*(17), doi:10.1029/2006gl027114.

Ruiz-Alvarez, O., V. P. Singh, J. Enciso-Medina, C. Munster, R. Kaiser, R. Ernesto Ontiveros-Capurata, L. Antonio Diaz-Garcia, and C. A. Costa dos Santos (2019), Spatio-temporal trends in monthly pan evaporation in Aguascalientes, Mexico, *Theoretical and Applied Climatology*, *136*(1-2), 775-789, doi:10.1007/s00704-018-2491-8.

Shimi, M., M. Najjarchi, K. Khalili, E. Hezavei, and S. M. Mirhoseyni (2020), Investigation of the accuracy of linear and nonlinear time series models in modeling and forecasting of pan evaporation in IRAN, *Arabian Journal of Geosciences*, *13*(2), doi:10.1007/s12517-019-5031-7.

Stephens, C. M., T. R. McVicar, F. M. Johnson, and L. A. Marshall (2018), Revisiting Pan Evaporation Trends in Australia a Decade on, *Geophysical Research Letters*, *45*(20), doi:10.1029/2018gl079332.

Talaee, P. H., H. Tabari, and H. Abghari (2014), Pan evaporation and reference evapotranspiration trend detection in western Iran with consideration of data persistence, *Hydrology Research*, *45*(2), 213-225, doi:10.2166/nh.2013.058.

Topaloglu, F., M. Ozfidaner, and F. Aydin (2012), Regional trends in Turkish pan evaporation, *Journal of Food Agriculture & Environment*, *10*(3-4), 960-962.

Verma, I. J., and V. N. Jadhav (2008), Recent variations and trends in pan evaporation over India, *Mausam*, *59*(3), 347-356.

Vicente-Serrano, S. M., et al. (2018), A comparison of temporal variability of observed and model-based pan evaporation over Uruguay (1973-2014), *International Journal of Climatology*, *38*(1), 337-350, doi:10.1002/joc.5179.

Wang, K., X. Liu, Y. Li, X. Yang, P. Bai, C. Liu, and F. Chen (2019), Deriving a long-term pan evaporation reanalysis dataset for two Chinese pan types, *Journal of Hydrology*, *579*, doi:10.1016/j.jhydrol.2019.124162.

Wang, T., J. Zhang, F. Sun, and W. Liu (2017), Pan evaporation paradox and evaporative demand from the past to the future over China: a review, *Wiley Interdisciplinary Reviews: Water*, *4*(3), doi:10.1002/wat2.1207.

Xie, B., Q. Zhang, and Y. Ying (2011), Trends in Precipitable Water and Relative Humidity in China: 1979–2005, *Journal of Applied Meteorology Climatology*, *50*(10), 1985-1994.

Xiong, A.-Y., J. Liao, and B. Xu (2012), Reconstruction of a Daily Large-Pan Evaporation Dataset over China, *Journal of Applied Meteorology and Climatology*, *51*(7), 1265-1275, doi:10.1175/jamc-d-11-0123.1.

Yagbasan, O., V. Demir, and H. Yazicigil (2020), Trend Analyses of Meteorological Variables and Lake Levels for Two Shallow Lakes in Central Turkey, *Water*, *12*(2), doi:10.3390/w12020414.

Yang, H., and D. Yang (2012), Climatic factors influencing changing pan evaporation across China from

1961 to 2001, *Journal of Hydrology*, *414-415*, 184-193, doi:10.1016/j.jhydrol.2011.10.043.
Yang, Y., N. Zhao, X. Hao, and C. Li (2009), Decreasing trend of sunshine hours and related driving forces in North China, *Theoretical Applied Climatology*, *97*(1-2), 91-98.
Yang, Z. B., Z. H. Li, and J. He (2014), Impact assessment of replacement of temperature and humidity sensor in automatic meteorological station, *Journal of Applied Meteorological Science*, *25*(2), 9-16.

Table lists

Table 1 Recent change in the pan evaporation trend in certain regions.

Table 2 Standard deviation in the conversion coefficient at the stations.

Table 3 Contribution of the climatic factors to the nationwide annual E_{pan} trends.

Table 4 Comparison of the pan evaporation trends.

Table 5 Attribution analysis of the change trend in pan evaporation at the stations controlled by the wind speed (mm/a/a).

Table 1. Recent change in the pan evaporation trend in certain regions.

Period	Study area (station numbers)	Pan evaporation trend (mm/a/a)	Reference
1970-2002	Australia (30)	-4.3	Roderick and Farquhar (2004)
1975-2016	Australia (37)	More stations exhibit a positive trend than from 1975-2004	Stephens et al. (2018)
1975-2006	Turkey (66)	Fifty stations reveal an increasing trend while 16 stations exhibit a nonsignificant decreasing trend	Topaloglu et al. (2012)
1997-2015	Turkey (-)	-0.1	Yagbasan et al. (2020)
1982-2003	Iran (31)	Significant decreasing trend	Talaee et al. (2014)
1995-2015	Iran (12)	16.0	Shimi et al. (2020)
1960-1990	Mexico (150)	-3.8	Ruiz-Alvarez et al. (2019)
1990-2010		-2.6	
1960-1993	China (-)	-2.6	Wang et al. (2017)
1994-2014		4.3	
1960-1991	China (518)	-5.4	Liu et al. (2016)
1992-2007		7.9	

Table 2. Standard deviation in the conversion coefficient at the stations.

Month	Station Numbers	STD<0.2	0.2<STD<0.4	STD>0.4
January	219	79.9%	17.8%	2.3%
February	226	88.1%	11.5%	0.4%
March	270	90.0%	9.6%	0.4%
April	360	96.1%	3.9%	0.0%
May	462	96.1%	3.7%	0.2%
June	465	95.1%	4.7%	0.2%
July	465	93.8%	6.0%	0.2%
August	465	97.6%	2.2%	0.2%
September	465	96.6%	3.0%	0.4%
October	400	93.0%	6.5%	0.5%
November	317	90.6%	8.8%	0.6%
December	242	88.8%	9.5%	1.7%

Table 3. Contribution of the climatic factors to the nationwide annual E_{pan} trends.

Elements	RH			SSD			T			U			$\frac{dE_{pan}}{dt}\|_{cal}$ mm/a/a	$\frac{dE_{pan}}{dt}\|_{obs}$ mm/a/a
	$\frac{dRH}{dt}$ %/a	ε_1 mm/a/%	RH^* mm/a/a	$\frac{dSSD}{dt}$ h/a	ε_2 mm/a/h	SSD^* mm/a/a	$\frac{dT}{dt}$ °C/a	ε_3 mm/a/°C	T^* mm/a/a	$\frac{dU}{dt}$ m/s/a	ε_4 mm/a/m/s	U^* mm/a/a		
Original	-0.11	-17.90	2.02		0.18	-0.29		153.4	4.66		590.22	-2.67	3.72	
Modified-1%	-0.06	-17.90	1.13	1.6	0.18	-0.29	0.03	153.5	4.66	0.005	582.31	-2.64	2.87	2.68
Modified-2%	-0.01	-17.91	0.24		0.18	-0.29		153.6	4.67		574.40	-2.60	2.01	

Table 4. Comparison of the pan evaporation trends.

Period	Trend according to the D20 dataset in this study	Trend simulated by the PenPan-D20 model in this study	Trend reported in previous studies
1994-2014	1.4 mm/a/a	3.1 mm/a/a	4.3 mm/a/a (*T Wang et al.*, 2017) and 5.2 mm/a/a (*K Wang et al.*, 2019)
1992-2007	7.7 mm/a/a	9.1 mm/a/a	10.1 mm/a/a (*K Wang et al.*, 2019)

Table 5. Attribution analysis of the change trend in pan evaporation at the stations controlled by the wind speed (mm/a/a).

Station	RH^*	SSD^*	T^*	U^*	Trend
50425	1.61	0.02	-0.42	2.60	3.81
50468	0.65	-0.72	0.75	-3.88	-3.20
52859	1.55	-0.18	5.86	-9.86	-2.63
53963	4.43	-2.89	6.88	-8.07	0.35
54186	2.43	-0.98	2.36	-3.74	0.07
55279	3.10	-0.74	6.30	-8.41	0.25
56586	2.01	1.08	3.71	-4.86	1.94

Figure lists

Figure 1 Number of usable stations with D20 and E601 observations.

Figure 2 Distribution of the meteorological stations used in this study.

Figure 3 Comparison of the monthly D20 observations to the estimation using the conversion coefficient method: calibration (left) and validation (right).

Figure 4 Nationwide annual trends of the (a) relative humidity (the black line represents the original humidity data, the blue line represents the modified-1% relative humidity, and the red line represents the modified-2% relative humidity), (b) sunshine duration, (c) air temperature, and (d) wind speed, from 1988-2017 (except for the modified-2% relative humidity, all the other trends are at least significant at P=0.05).

Figure 5 (a) Nationwide annual trend of the pan evaporation, (b) change trend in the pan evaporation detected by the MK test at a significance level of P=0.05. The red/blue triangles represent the stations with significant increasing/decreasing trends, while the circles represent the stations with no significant trends.

Figure 6 Nationwide annual E_{pan} trends from 1988-2017. The black, blue, and red lines represent the E_{pan} values derived from the original humidity data (P<0.001), the modified-1% relative humidity (P<0.001), and the modified-2% relative humidity (P<0.01), respectively.

Figure 7 Controlling climatic factors of the E_{pan} change at the 469 stations across China.

Figure 8 Difference between the annual D20 observations and annual D20 simulations according to the PenPan-20 model. The dotted lines represent the mean average values during the two periods, namely, 1988-2003 and 2004-2017.

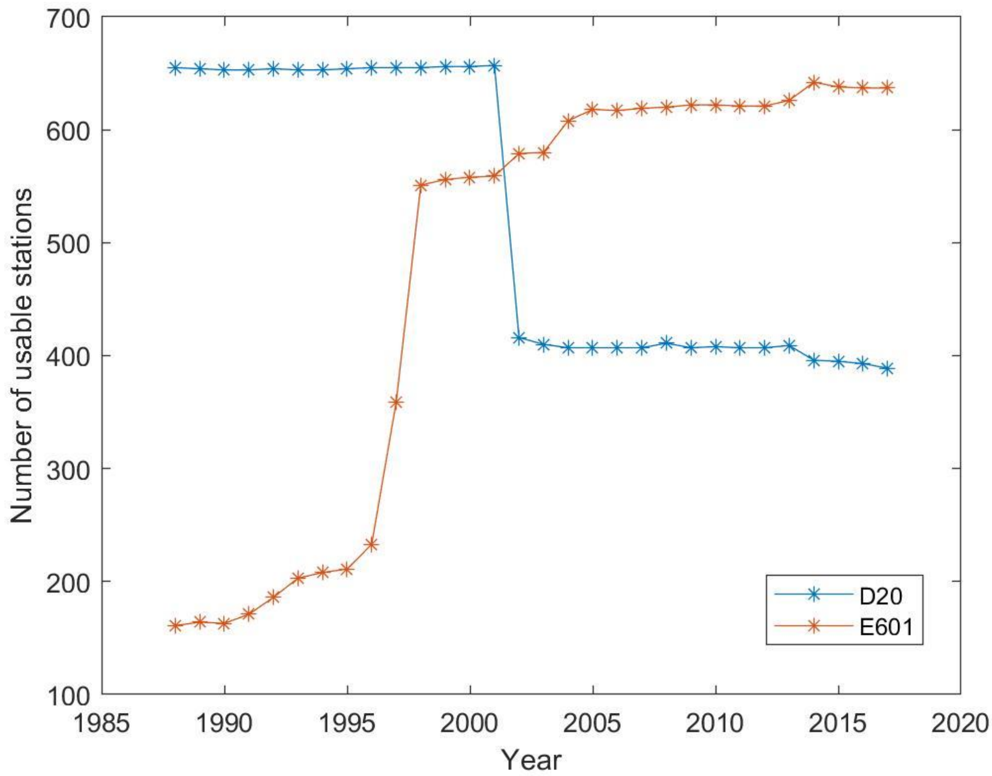

Figure 1. Number of usable stations with D20 and E601 observations.

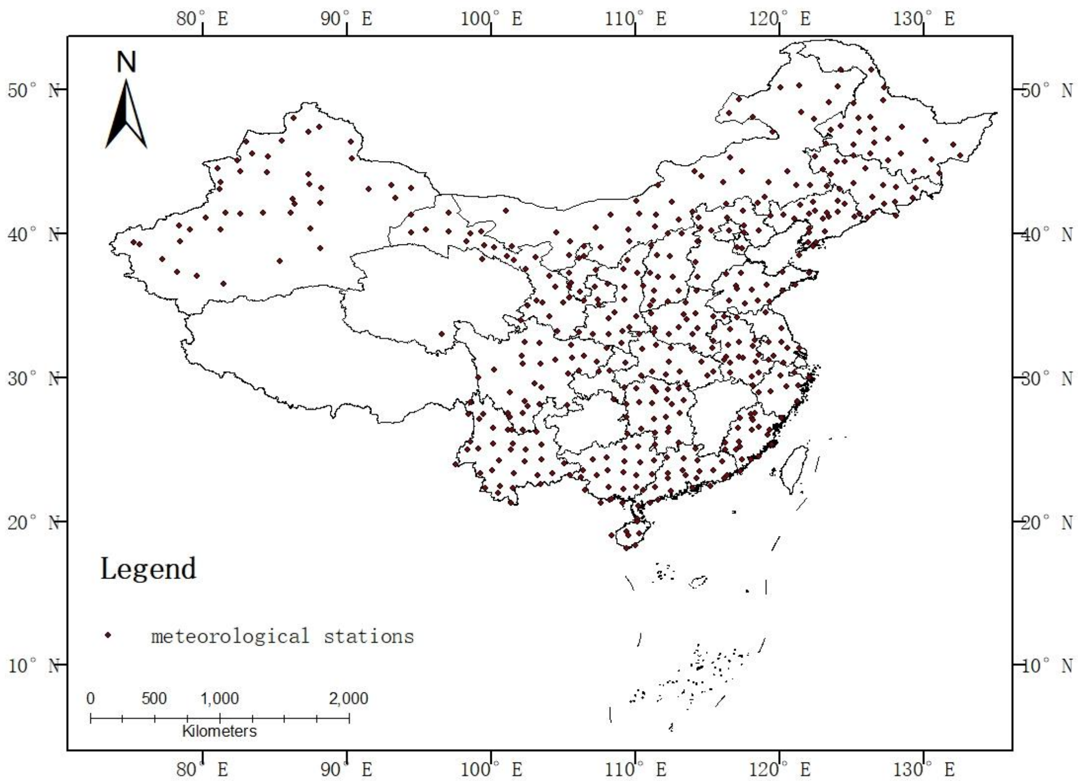

Figure 2. Distribution of the meteorological stations used in this study.

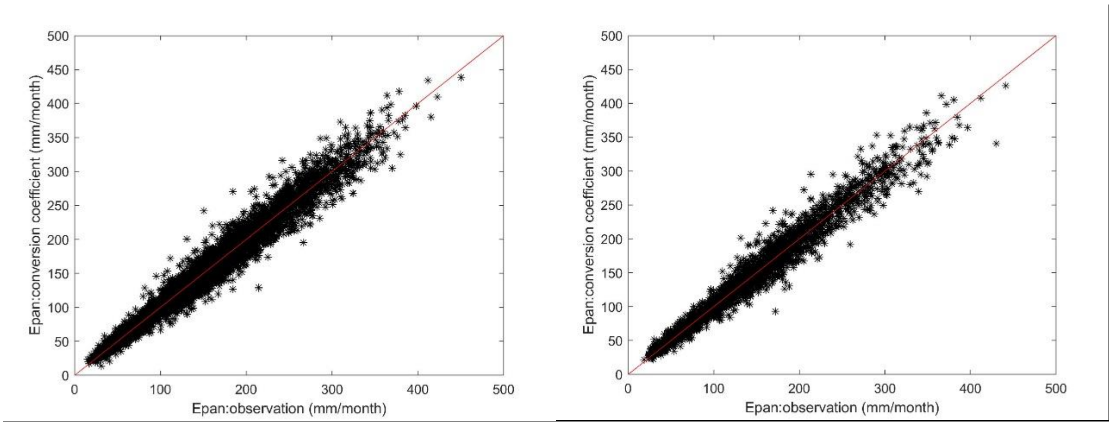

Figure 3. Comparison of the monthly D20 observations to the estimation using the conversion coefficient method: calibration (left) and validation (right).

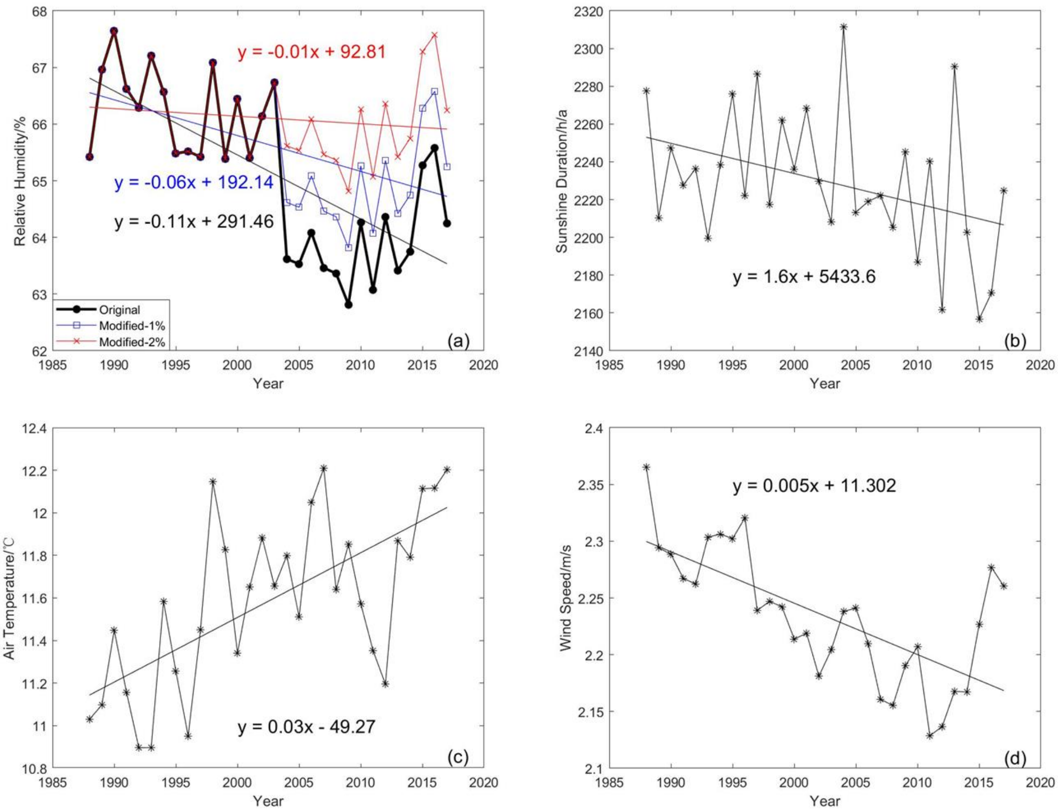

Figure 4. Nationwide annual trends of the (a) relative humidity (the black line represents the original humidity data, the blue line represents the modified-1% relative humidity, and the red line represents the modified-2% relative humidity), (b) sunshine duration, (c) air temperature, and (d) wind speed, from 1988-2017 (except for the modified-2% relative humidity, all the other trends are at least significant at P=0.05).

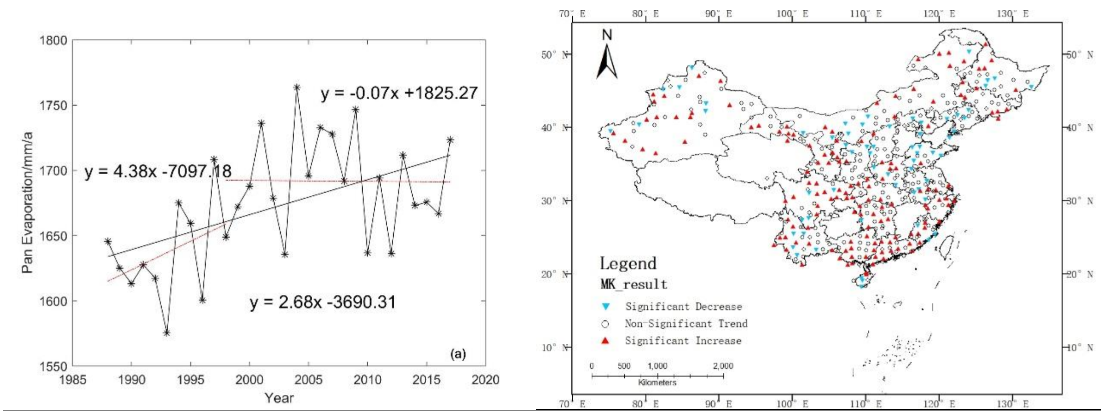

Figure 5. (a) Nationwide annual trend of the pan evaporation, (b) change trend in the pan evaporation detected by the MK test at a significance level of P=0.05. The red/blue triangles represent the stations with significant increasing/decreasing trends, while the circles represent the stations with no significant trends.

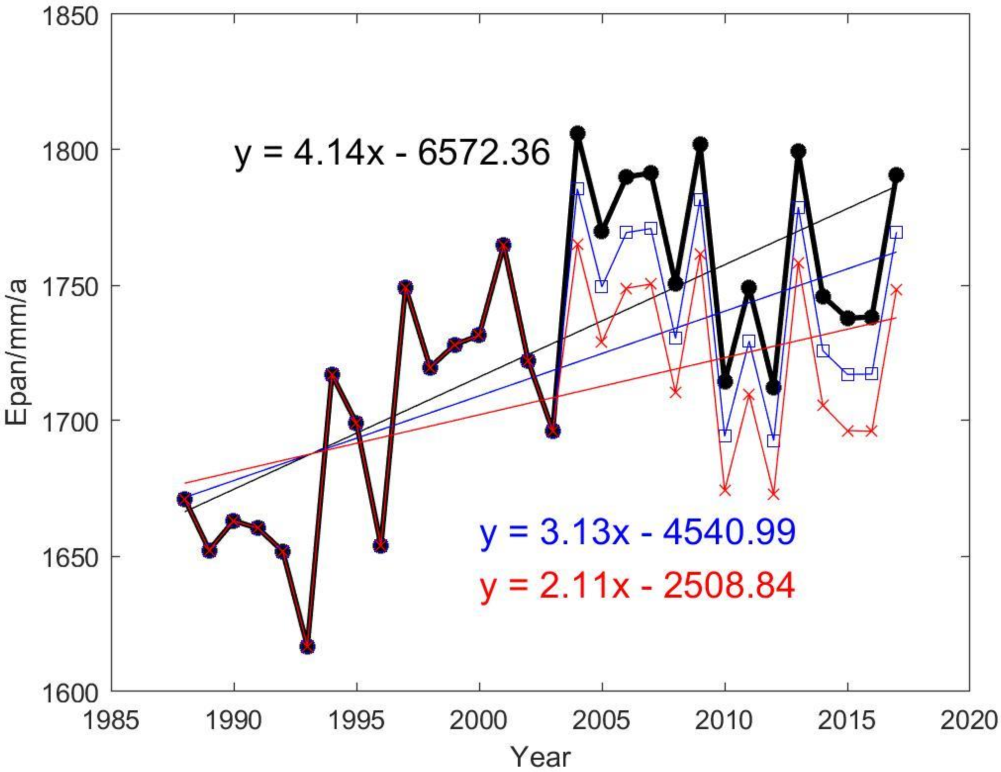

Figure 6. Nationwide annual E_{pan} trends from 1988-2017. The black, blue, and red lines represent the E_{pan} values derived from the original humidity data (P<0.001), the modified-1% relative humidity (P<0.001), and the modified-2% relative humidity (P<0.01), respectively.

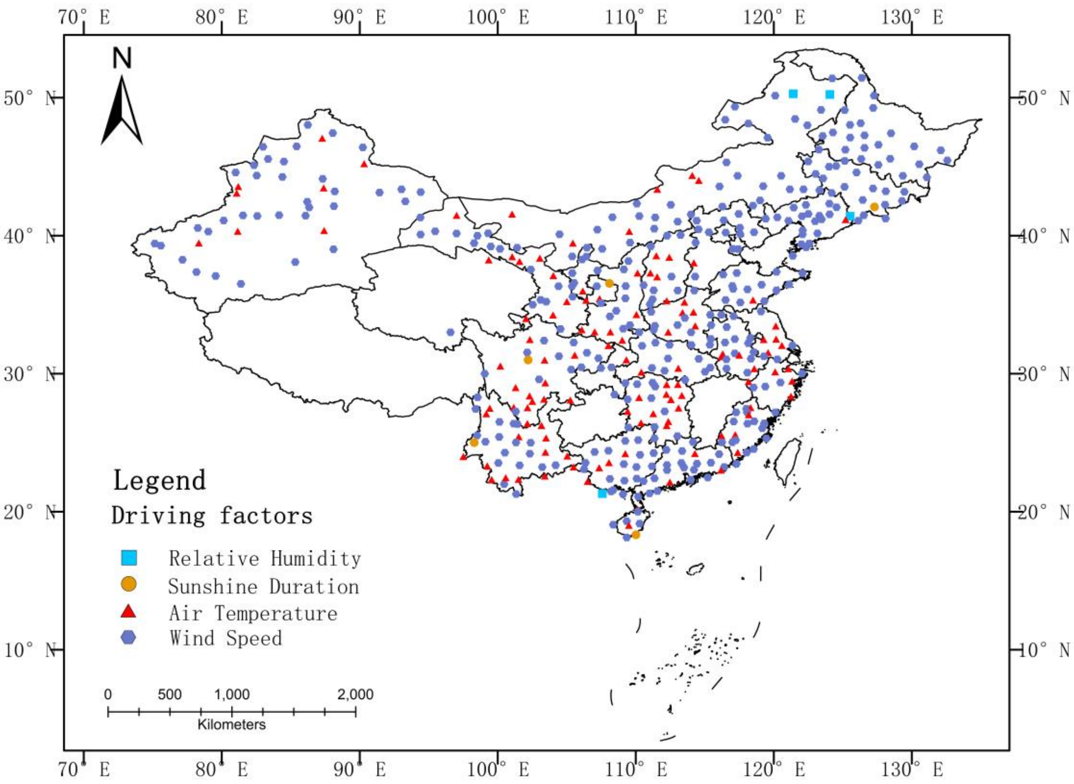

Figure 7. Controlling climatic factors of the E_{pan} change at the 469 stations across China.

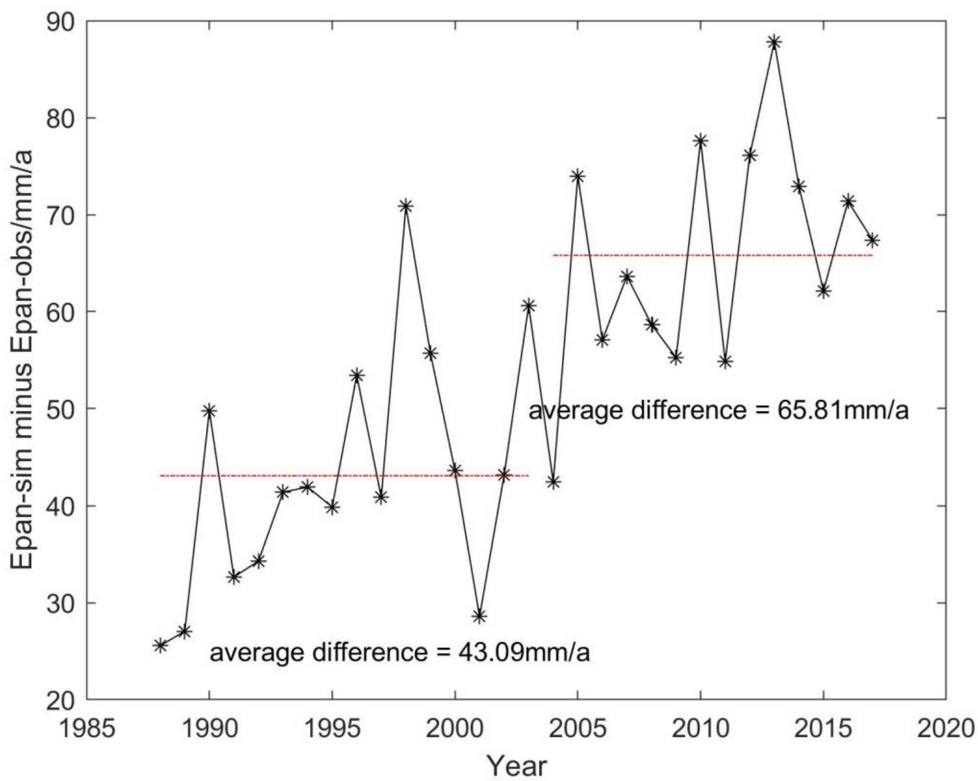

Figure 8. Difference between the annual D20 observations and annual D20 simulations according to the PenPan-20 model. The dotted lines represent the mean

average values during the two periods, namely, 1988-2003 and 2004-2017.